

Characterization of Water-Soluble Ions in PM_{2.5} in Chongqing, a Megacity in Eastern Sichuan Basin, China

Tianli Song¹, Xuyao Cao^{2,3,#}, Huanbo Wang⁴, Yang Qiu¹, Yang Chen⁶, Mi Tian^{5,*}, Jianyan Yu⁶, Chongzhi Zhai⁷, Fumo Yang^{1,*}

¹Department of Environmental Science and Engineering, Sichuan University, Chengdu, 610065, China

²Railway Engineering Consulting Group Co., LTD., Beijing, 100055, China

³Research Center for Atmospheric Environment, Chongqing Institute of Green and Intelligent Technology, Chinese Academy of Sciences, Chongqing 400714, China

⁴School of Environment and Resource, Southwest University of Science and Technology, Mianyang, 621010, China

⁵School of Environment and Ecology, Chongqing University, Chongqing, 400044, China

⁶Chongqing Monitoring Center for Ecology and Environment, Chongqing 401147, China

⁷Chongqing Academy of Environmental Science, Chongqing 401147, China

Abstract: Samples of PM_{2.5} were collected at three urban sites and one rural site simultaneously in Chongqing, the only megacity in eastern Sichuan Basin, Southwest China, from October 15 to November 13, 2015. Water-soluble ions (WSIs, i.e., F⁻, Cl⁻, NO₃⁻, SO₄²⁻, K⁺, Na⁺, NH₄⁺, Mg²⁺ and Ca²⁺) in PM_{2.5} were measured to investigate their characteristics and formation pathways. The average concentrations of PM_{2.5} at the urban sites were 55.5–59.0 μg m⁻³, which was 62.8–73.0% higher than that at rural site. SO₄²⁻, NO₃⁻, NH₄⁺ were the dominant ions, contributing to more than 90% of total WSIs. The coefficients of divergence for SO₄²⁻ between the urban and rural sites were 0.15–0.17, indicating its relatively uniform distribution across Chongqing. Analysis of the formation mechanisms of SO₄²⁻ and NO₃⁻ in PM_{2.5} suggested that the heterogeneous reaction was responsible for the high concentrations of sulfate among the four sites, whereas nitrate was formed mainly through homogeneous reactions at the urban sites. Furthermore, the results of trajectory clustering showed that the air pollution were mainly from local sources within the basin. Our findings on PM_{2.5} composition in Chongqing help to advance the knowledge on PM_{2.5} pollution in Chinese megacities, and to provide more evidence for further pollution mitigation.

Keywords: PM_{2.5}, Water-soluble ions, Formation pathway, Chongqing, Sichuan basin.

1. INTRODUCTION

Fine particulate matter with diameter of 2.5 micrometers or less (PM_{2.5}) is of wide public concern. The chemical compositions of PM_{2.5} are closely associated with its effects on human health and atmospheric visibility [1]. Water soluble ions (WSIs) are major components of PM_{2.5}, accounting for up to 60–70% of PM_{2.5} mass in some cities [2, 3]. Sulfate (SO₄²⁻), nitrate (NO₃⁻) and ammonia (NH₄⁺) are secondary inorganic aerosols (collectively known as SNA) and are the dominant ionic species in PM_{2.5}, accounting for more than 80% of total WSIs [2, 4, 5]. Due to their strong hygroscopicity, SNA have significant influence on extinction coefficient and atmospheric visibility [6–8]. Also, acidic components (i.e., SO₄²⁻ and NO₃⁻) and alkaline species (i.e., NH₄⁺) determine the acidity of PM_{2.5}, a chemical feature that

can bring greater impact on the ecosystem and environmental conditions through acid deposition [9].

Chongqing, nicknamed as the “mountain city”, is located in the eastern margin of Sichuan Basin, which is surrounded by 1000–3000 meters high mountains and plateaus. Due to local topography, the average near-surface wind speed in Chongqing is 0.7–1.7 m/s and the annual average temperature is ordinarily above 18 °C [10]. Additionally, rainfall between May and September accounts for 70% of annual precipitation. Thus, humidity is high (annual average: > 70%) in Chongqing, attributed by the abundant water resource and warm weather. These specific geographical and meteorological conditions favor the accumulation of pollutants, potentially contributing to the formation of secondary particulate matter. Though strict emission controls have been implemented all around China since 2013 [11], primary particulates and gaseous precursors emissions remain at a high level in Chongqing. For example, the emissions of SO₂, NO_x, fume and dust from industry in 2014 in Chongqing were 47.5×10⁴ tons, 23.4×10⁴ tons, 21.5×10⁴ tons,

*Address correspondence to these author at the Department of Environmental Science and Engineering, Sichuan University, Chengdu, 610065, China; Tel: +86-28-8540-4973;

E-mail: fmyang@scu.ac.cn; tianmi628@cqu.edu.cn

#Contributed equally with the first author to this work

respectively, ranking first among 31 provincial capitals and direct administrative cities in China [10, 12]. Persistent high pollutant emission plays a critical role in the mass concentration and ionic composition of PM_{2.5} in Chongqing.

In this study, PM_{2.5} samples were collected at four sites in Chongqing between October and November of 2015. The samples were analyzed for mass concentrations and chemical compositions. The spatial-temporal variability of SNA and the formation mechanisms of SO₄²⁻ and NO₃⁻ were investigated to understand the characterization of PM_{2.5} and its major ionic species. In addition, cluster analysis of backward trajectories was applied to identify the possible transport pathway of air pollution in Chongqing.

2. MATERIALS AND METHODS

2.1. Sampling Sites

Aerosol sampling was conducted at four sites in Chongqing, including three urban sites, Jiefangbei (JFB), Shapingba (SPB), Yubei (YB), and one rural background site, Jinyun Mountain (JY), from October 15 to November 13, 2015 (Figure 1). The sampling site at JFB is located on the roof of the Second Affiliated Hospital of Chongqing Medical University, which is located at the center of Chongqing city surrounded by densely populated business districts. SPB site is located on the roof of the Seventh Middle School of

Chongqing, which is located in a mixed zone area comprised of schools, commercial buildings and residential buildings. YB site is located on Huangshan road (a main road) and close to highways (within 200 meters), which is surrounded by densely occupied office buildings. The rural site (JY) is located on the top of an abandoned hotel at Jinyun Mountain with flourishing vegetations, which is located approximately 35 km northwest of Chongqing city center and 5 km away from the nearest town (Beibei) [13].

2.2. Sample Collection and Analysis

PM_{2.5} samples were simultaneously collected from all four sites on both quartz (Whatman, England) and Teflon filters (Whatman, England) from 12:00 am to 10:00 am the next day with two mini volume samplers (Table 1). The hourly data of PM_{2.5}, PM₁₀, gaseous pollutants (SO₂, NO₂, O₃, and CO) and meteorological parameters for JFB, SPB and JY sites were also obtained from Chongqing Ecology and Environment Bureau.

PM_{2.5} mass concentrations were obtained by weighing the Teflon filters before and after sampling using an electronic microbalance with a sensitivity of ±0.001 mg (Sartorius ME5-F, Germany). Before weighing, the sample filters were equilibrated at a temperature of 20±5 °C and at a relative humidity (RH) of 40±5% for 24 hours.



Figure 1: Locations of sampling sites in Chongqing.

Table 1: Brief Introduction of PM_{2.5} Samplers

		JFB	SPB	YB	JY
Quartz filter samplers	Model	Partisol 2000i air samplers (Thermo Scientific, USA)	URG 3000ABC aerosol sampler (URG, USA)	Partisol 2000i air samplers (Thermo Scientific, USA)	frmOmni Ambient air sampler (BGI, USA)
	Flow rate	16.7 L/min	16.7 L/min	16.7 L/min	5 L/min
Teflon filter samplers	Model	frmOmni Ambient air sampler (BGI, USA)	URG 3000ABC aerosol sampler (URG, USA)	frmOmni Ambient air sampler (BGI, USA)	frmOmni Ambient air sampler (BGI, USA)
	Flow rate	5 L/min	16.7 L/min	5 L/min	5 L/min

One-fourth of each quartz filter was cut to analysis water-soluble ions. Five cations (Na^+ , K^+ , NH_4^+ , Mg^{2+} , and Ca^{2+}) and four anions (F^- , Cl^- , NO_3^- , and SO_4^{2-}) were determined by ion chromatograph (IC, Dionex 600, US). The detection limits were determined as the mean filed blank concentrations plus three times the standard deviation (3σ) of the field blanks [14], which corresponds to a range of 0.009–0.022 mg/L for anions and 0.005–0.090 mg/L for cations. Quality assurance and quality control (QA/QC) procedures for sample pretreatment, instrument analysis, and data processing followed our previous study [15].

2.3. Pearson Correlations and Coefficients of Divergence

Pearson correlations and coefficients of divergence (COD) have been used to evaluate the spatial distribution of SNA among different sampling sites [16]. The COD is calculated as follows:

$$\text{COD}_{jk} = 1 - \frac{1}{s} \sum_{i=1}^s \frac{N_{ij} - N_{ik}}{N_{ij} + N_{ik}} \quad (1)$$

Where N_{ij} and N_{ik} represent the concentration of i species measured at site j and k , and s is the number of samples. Generally, $\text{COD} < 0.2$ indicates a relatively similar spatial distribution [15, 17].

2.4. In-Situ Aerosol Acidity

Aerosol acidity is an important parameter influencing atmospheric chemistry and physics [2]. In general, both total acidity ($[\text{H}^+]_{\text{total}}$) and in-situ acidity ($[\text{H}^+]_{\text{in-situ}}$) were used as indicators of aerosol acidity [2, 9]. $[\text{H}^+]_{\text{total}}$ is the absolute acidity of aerosol, determined by total acids in aqueous extracts of filter samples. $[\text{H}^+]_{\text{in-situ}}$ is the actual acidity in the deliquesced aerosol, which influences the complex real-time reactions in atmospheric chemistry. $[\text{H}^+]_{\text{total}}$ was calculated using the following equation:

$$[\text{H}^+]_{\text{total}} = 2 \times [\text{SO}_4^{2-}] + [\text{NO}_3^-] - [\text{NH}_4^+] \quad (2)$$

where the mole concentrations of all the parameters was used.

In-situ acidity was estimated by AIM-II (Extended Aerosol Inorganic Model II) in the mixing system $\text{H}^+ - \text{NO}_3^- - \text{SO}_4^{2-} - \text{NH}_4^+ - \text{H}_2\text{O}$ [18]. The AIM-II is a state-of-art model, which can estimate aerosol acidity, aqueous-phase and solid-phase ionic components in the in-situ aerosols at variable temperature and RH [19]. The model input of AIM-II includes temperature, RH, $[\text{SO}_4^{2-}]$, $[\text{NO}_3^-]$, $[\text{NH}_4^+]$ and $[\text{H}^+]_{\text{total}}$. It should be noted that this model neglects the influence of organics on water uptake and on the partitioning of the inorganic species [20]. The aerosol pH was calculated as:

$$\text{pH} = -\log a_{\text{H}^+} = -\log \gamma_{\text{H}^+} \times [\text{H}^+]_{\text{in-situ}} \times 1000 \times \rho / m \quad (3)$$

where a_{H^+} is the activity of aqueous phase H^+ in the particle in the unit of mol/L, γ_{H^+} is the activity coefficient of $[\text{H}^+]_{\text{in-situ}}$, $[\text{H}^+]_{\text{in-situ}}$ is the concentration of free aqueous phase H^+ in the unit of mol/m³, ρ is the aerosol aqueous phase density in g/cm³, and m is the sum of mass concentrations of all ionic solutes in the aqueous phase plus. The parameters, *i.e.*, ρ , γ_{H^+} , $[\text{H}^+]_{\text{in-situ}}$ and aerosol liquid water content (LWC), are derived from AIM-II model.

2.5. Air Mass Back-Trajectory Cluster Analysis

To better understand the influence of regional transport on air pollution in urban Chongqing, 48-hour backward trajectories for JFB site were calculated using the TrajStat software [21, 22]. The meteorological input was adopted from the National Oceanic and Atmospheric Administration (NOAA) Air Resource Laboratory Archived Global Data Assimilation System (GDAS) [23]. The trajectories started from 2:00 UTC (10:00 local time) during the sampling period, which is consistent with the end time of each sampling day. Considering the planetary boundary layer height of Chongqing was generally low, the arrival heights of all the trajectories were set at 300 meters above ground

level [4]. Cluster analysis was also applied to identify the common atmospheric transport pathway arriving at JFB site.

3. RESULTS AND DISCUSSION

3.1. Concentration and Composition of PM_{2.5}

The concentrations of PM_{2.5} and nine water-soluble ions at all four sampling sites in this study are summarized (Table 2) and the daily trends of PM_{2.5} mass concentrations and major ionic species are also depicted (Figure 2). The daily concentrations of PM_{2.5} varied similarly at all the three urban sites with their average concentrations ranging from 55.5 to 59.0 $\mu\text{g}/\text{m}^3$, which were 62.8 to 73.0% higher than that at the rural site (34.1 $\mu\text{g}/\text{m}^3$). PM_{2.5} mass concentration at rural JY was substantially lower than that measured a decade ago (105 $\mu\text{g}/\text{m}^3$) [24], which should be attributed to the municipality's continued efforts to improve air quality in recent years. As shown in Figure 2, PM_{2.5} concentration peaked at 101 $\mu\text{g}/\text{m}^3$ on October 24 at JFB when SO₄²⁻ concentration was at the

highest, while the highest concentrations of NO₃⁻ and NH₄⁺ were observed on October 19.

Among the three urban sites, the average concentrations of total WSIs was 21.5–23.8 $\mu\text{g}/\text{m}^3$, accounting for 38.8–40.8% of PM_{2.5}. Rural JY site reported the lowest average concentration of total WSI (14.9 $\mu\text{g}/\text{m}^3$), and this concentration ranks the highest in terms of percentage contribution to PM_{2.5} (43.5%). SO₄²⁻, NO₃⁻ and NH₄⁺ were the major components of WSIs, and the total concentration of these three ions contributed to more than 90% of total WSIs among the four sampling sites. SO₄²⁻ (8.09–10.1 $\mu\text{g}/\text{m}^3$) was the most abundant ionic species, followed by NO₃⁻ (3.39–6.13 $\mu\text{g}/\text{m}^3$) and NH₄⁺ (2.48–5.53 $\mu\text{g}/\text{m}^3$), which is similar to our previous studies in urban and rural areas of Chongqing conducted in autumn 2014 [13, 25]. The average concentrations of SO₄²⁻ in urban Chongqing are significantly lower than that in autumn 2012 (average: 15.4 $\mu\text{g}/\text{m}^3$), whereas NO₃⁻ and NH₄⁺ are comparable to those during the same period (8.4 and 6.9 $\mu\text{g}/\text{m}^3$, respectively) [26]. The sharp decrease in

Table 2: Summary of Water-Soluble Ions and Acidity in PM_{2.5} and Meteorological Data among Four Sites in Chongqing

	JFB	SPB	YB	JY
PM _{2.5} ($\mu\text{g}/\text{m}^3$)	57.1±19.5	59.0±19.9	55.5±17.4	34.1±13.6
SO ₄ ²⁻ ($\mu\text{g}/\text{m}^3$)	9.93±4.71	10.1±4.69	9.52±4.31	8.09±3.16
NO ₃ ⁻ ($\mu\text{g}/\text{m}^3$)	6.13±3.80	6.01±3.12	5.40±3.03	3.39±1.69
NH ₄ ⁺ ($\mu\text{g}/\text{m}^3$)	5.53±2.95	5.01±2.42	4.86±2.28	2.41±1.54
F ⁻ ($\mu\text{g}/\text{m}^3$)	0.04±0.02	0.03±0.02	0.04±0.03	NA ^a
Cl ⁻ ($\mu\text{g}/\text{m}^3$)	0.86±0.70	0.67±0.46	0.44±0.31	0.24±0.12
Na ⁺ ($\mu\text{g}/\text{m}^3$)	0.62±0.22	0.60±0.30	0.53±0.16	0.51±0.39
K ⁺ ($\mu\text{g}/\text{m}^3$)	0.60±0.27	0.67±0.28	0.55±0.24	0.30±0.23
Mg ²⁺ ($\mu\text{g}/\text{m}^3$)	0.03±0.01	0.03±0.02	0.03±0.01	0.01±0.05
Ca ²⁺ ($\mu\text{g}/\text{m}^3$)	0.08±0.09	0.12±0.09	0.17±0.12	0.08±0.21
Total ions ($\mu\text{g}/\text{m}^3$)	23.8±11.5	23.3±9.88	21.5±8.96	14.9±5.75
SNA/ Total ions (%)	90.1±2.50	90.4±2.99	90.9±3.76	93.2±2.94
Total ions/PM _{2.5} (%)	40.8±11.4	39.4±9.46	38.8±10.3	43.5±7.67
NO ₃ ⁻ /SO ₄ ²⁻ (mass ratio)	0.65±0.30	0.64±0.30	0.62±0.32	0.45±0.23
[H ⁺] _{total} (nmol/m ³)	14.8±16.2	30.8±21.4	19.8±8.67	90.7±33.7
[H ⁺] _{in-situ} (nmol/m ³)	3.14±7.39	5.84±5.74	4.64±2.98	41.5±29.3
[HSO ₄ ⁻] (nmol/m ³)	11.7±10.0	25.1±17.0	15.2±7.14	46.4±10.5
pH	0.81±0.99	0.92±0.76	1.01±0.65	~0.11±0.50
LWC ($\mu\text{g}/\text{m}^3$)	8.09±5.02	28.5±23.0	33.5±29.6	29.2±16.0
T (°C)	19.5±2.89	18.6±2.83	16.8±3.26	14.4±3.49
RH (%)	71.0±8.14	77.4±7.50	81.6±10.7	80.3±10.4

^anot detected in this study."

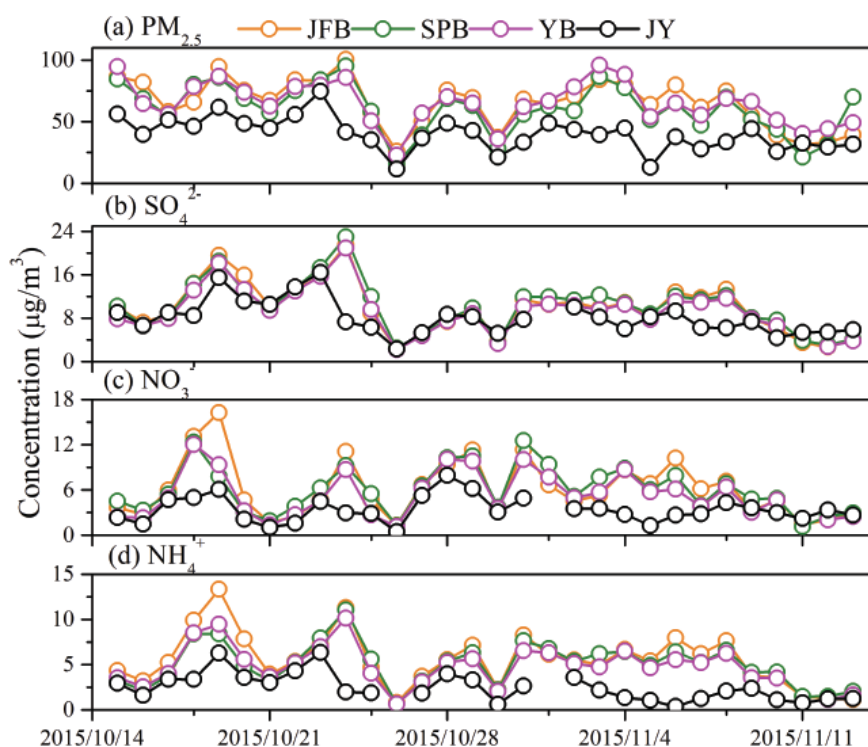


Figure 2: Daily variations of (a) $PM_{2.5}$ and (b-d) major ions among the four sampling sites.

SO_4^{2-} could be the result of the systematic installation of desulphurization system as part of the “Air Pollution Prevention and Control Action Plan” started in September 2013 [11].

The concentrations and temporal variations of SNA were similar among three urban sites, while lower concentrations were observed at JY site with slightly different temporal variation (Figure 2). As listed in Table 3, significant correlation ($r>0.85$, $p<0.01$) and extremely low COD values (0.05–0.13) were found for SNA among three urban sites, suggesting similar emission, accumulation and removal processes of those secondary ions in different areas of urban Chongqing. Meanwhile, relative high correlation coefficients ($r=0.79$ – 0.80 , $p<0.01$) and low COD (0.15–0.17) for SO_4^{2-} were observed between urban and rural sites. It suggests that SO_4^{2-} was homogeneously distributed regionally covering both urban and rural Chongqing. This is consistent with the spatial uniformity of annual average concentrations of SO_2 in 2015 (13–18 $\mu\text{g}/\text{m}^3$) over the nine urban districts with a whole area of about 5470 km^2 [27]. However, the high COD values (0.27–0.43) of NO_3^- and NH_4^+ between urban and rural sites might be influenced by the different contributions of local sources and different formation mechanisms of these species (see further discussion in the following sections).

3.2. Stoichiometric Analysis of Cations and Anions

As shown in Figure 3(a), strong correlations ($r>0.98$, $p<0.01$) were found between total anion equivalents ($\sum \text{anions}$) and total cation equivalents ($\sum \text{cations}$) with slope of the linear regressions (1.01–1.07) closed to 1.00 among the three urban sites, suggesting the aerosols were neutral in urban Chongqing. In contrast, a lower regression slope (0.73) was observed at JY site, demonstrating a deficiency of cations, which should be related to the acidic aerosols in rural Chongqing.

NH_4^+ is the protonation product of NH_3 and is the most abundant cation in aerosols. Generally, NH_4^+ exists in the forms of $(NH_4)_2SO_4$, NH_4HSO_4 , and NH_4NO_3 in $PM_{2.5}$, and much NH_4^+ exists in the aerosol in the forms of $(NH_4)_2SO_4$ or NH_4HSO_4 due to their stability and low volatility compared to NH_4NO_3 [7]. Figure 3(b) showed significant correlations between $2[SO_4^{2-}]$ and $[NH_4^+]$ (equivalent concentration, $\mu\text{eq}/\text{m}^3$). Almost all the points at the urban sites were above 1:1 line, which suggests that SO_4^{2-} was fully neutralized by NH_4^+ and mainly presented in the form of $(NH_4)_2SO_4$ [28]. We further considered the charge balance between NH_4^+ and the combination of SO_4^{2-} and NO_3^- , as depicted in Figure 3(c). Among the four sampling sites, significant correlations ($r>0.99$, $p<0.01$) were observed between $[NH_4^+]$ and $2[SO_4^{2-}]+[NO_3^-]$

Table 3: Pearson Correlations and Coefficients of Divergence (COD) for SNA Among Four Sampling Sites

	SO ₄ ²⁻	JFB	SPB	YB	JY	NO ₃ ⁻	JFB	SPB	YB	JY	NH ₄ ⁺	JFB	SPB	YB	JY
r	JFB	1				JFB	1				JFB	1			
	SPB	0.97	1			SPB	0.85	1			SPB	0.91	1		
	YB	0.99	0.99	1		YB	0.91	0.95	1		YB	0.97	0.97	1	
	JY	0.79	0.79	0.8	1	JY	0.65	0.69	0.72	1	JY	0.52	0.44	0.50	1
COD	SO ₄ ²⁻	JFB	SPB	YB	JY	NO ₃ ⁻	JFB	SPB	YB	JY	NH ₄ ⁺	JFB	SPB	YB	JY
	JFB	1				JFB	1				JFB	1			
	SPB	0.05	1			SPB	0.13	1			SPB	0.11	1		
	YB	0.05	0.06	1		YB	0.12	0.13	1		YB	0.1	0.07	1	
JY	0.17	0.17	0.15	1	JY	0.33	0.32	0.27	1	JY	0.43	0.41	0.39	1	

(μeq/m³), and the ratio of [NH₄⁺] to 2[SO₄²⁻]+[NO₃⁻] approximate 1.00 at JFB and YB sites, but SPB reported lower ratio (0.92) and more scattered points. JY site reported a relatively low ratio (0.67), suggesting different chemical forms of SNA at urban and/or rural Chongqing. To further examine the chemical forms of SNA, the theoretical mass concentration of NH₄⁺ was calculated. When NH₄⁺ exists as NH₄NO₃ and (NH₄)₂SO₄, the concentration of NH₄⁺ can be calculated by the following equation,

$$C_{cal1} = 0.29C_{NO3} + 0.38C_{SO4} \quad (4)$$

When NH₄⁺ exists as NH₄NO₃ and NH₄HSO₄, the concentration of NH₄⁺ can be calculated as,

$$C_{cal2} = 0.29C_{NO3} + 0.192C_{SO4} \quad (5)$$

The scatter plots for measured and the calculated concentrations are shown in Figure 3(d). Most of the points derived by Eq. (4) were close to the 1:1 line among the three urban sites, demonstrating sufficient

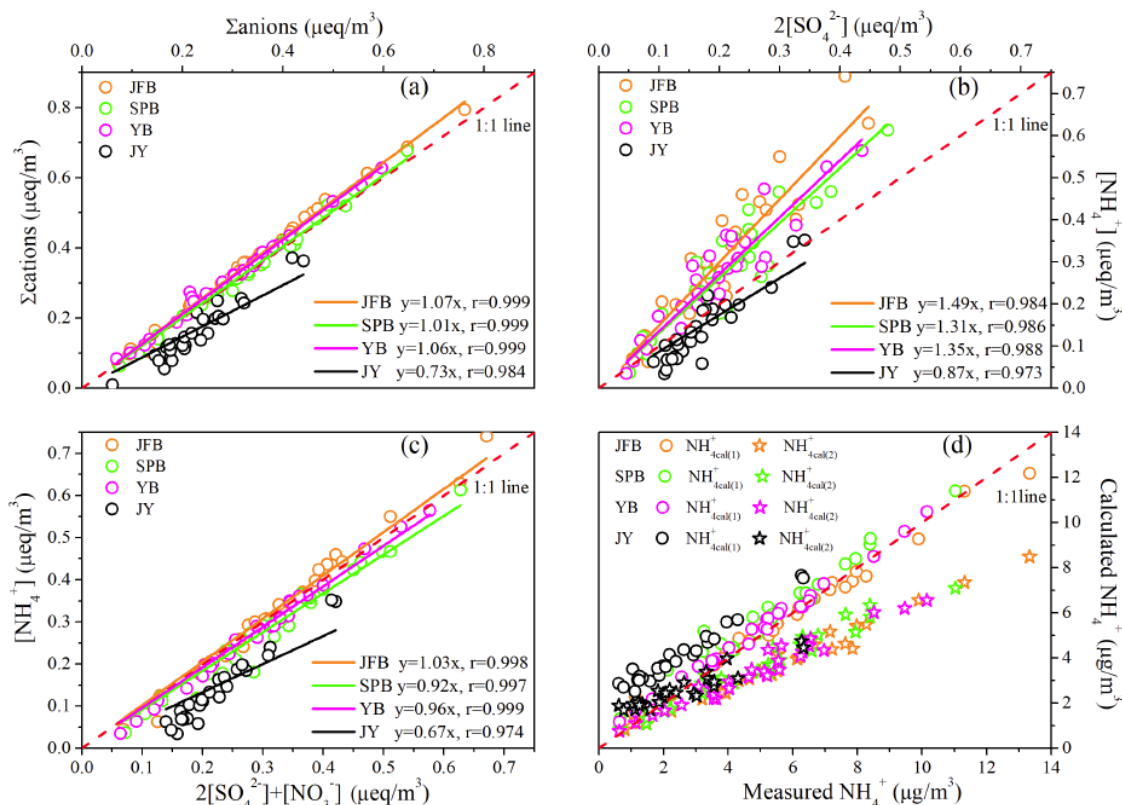


Figure 3: Correlations between: (a) total cations and anions, (b) [NH₄⁺] and [SO₄²⁻], (c) [NH₄⁺] and 2[SO₄²⁻]+[NO₃⁻], (d) calculated NH₄⁺ and measured NH₄⁺.

ammonium conditions in urban Chongqing and that SNA was mainly present in the forms of $(\text{NH}_4)_2\text{SO}_4$ and NH_4NO_3 . Points farther away from 1:1 line, especially at SPB site, are indicative of the existence of NH_4HSO_4 in urban Chongqing. For JY site, all the points derived from Eq. (4) were above the 1:1 line, suggesting the samples from JY site were ammonium-poor. When NH_4^+ was derived from Eq. (5), most of the points were above the 1:1 line, indicating SO_4^{2-} was mainly in the form of NH_4HSO_4 in rural Chongqing. However, there were also some points derived from Eq. (5) were under the 1:1 line. Thus, the existence of $(\text{NH}_4)_2\text{SO}_4$ should not be neglected in rural Chongqing.

3.3. Analysis of Aerosol Acidity

The equivalent charge ratio (eq/eq) of NH_4^+ to the sum of SO_4^{2-} and NO_3^- , which is expressed as $R = [\text{NH}_4^+] / (2 \times [\text{SO}_4^{2-}] + [\text{NO}_3^-])$, was used as the indicator of acidic property of $\text{PM}_{2.5}$ [9]. The $\text{PM}_{2.5}$ samples were divided into two groups with $R \leq 1$ being acidic aerosol, while $R > 1$ being alkaline. As shown in Figure 3 (c), the aerosols were more acidic at JY ($R = 0.67$) while less acidic at SPB ($R = 0.92$), and almost neutral at JFB ($R = 1.03$) and YB ($R = 0.96$).

To further explore aerosol acidity in Chongqing, more parameters related to aerosol acidity, such as $[\text{H}^+]_{\text{total}}$, $[\text{H}^+]_{\text{in-situ}}$ and pH, were calculated by AIM-II model. The input temperature and humidity are average values over the whole observation period. As shown in Table 2, the $[\text{H}^+]_{\text{total}}$ and $[\text{H}^+]_{\text{in-situ}}$ at rural site (JY) were much higher than those at the three urban sites, indicating that the aerosol in rural area was more acidic than urban areas in Chongqing, which may be related to less neutralization of H_2SO_4 and HNO_3 by NH_3 at the rural site.

As mentioned above, the samples at SPB and JY were acidic with high concentration of $[\text{H}^+]_{\text{total}}$ (30.8 and 90.7 nmol/m^3 , respectively), while samples at JFB and YB sites were almost neutral. Thus, the characteristics of aerosol acidity were further evaluated at these two sites. Generally, aerosol acidity was closely related to water content and chemical composition of $\text{PM}_{2.5}$. Higher levels of aerosol LWC promote H_2SO_4 and/or HSO_4^- to free more H^+ leading to higher in-situ acidity, but overall it dilutes the H^+ concentrations increasing the pH of the aerosols [29]. As listed in Table 2, although aerosol LWC and RH were comparable at JY and SPB sites, the acidic parameters (e.g., $[\text{H}^+]_{\text{in-situ}}$ and pH) were quite different. The $[\text{H}^+]_{\text{in-situ}}$ at JY was 41.5, much higher than that at SPB (5.84), suggesting that

the aerosol acidity was more related to the chemical composition rather than LWC and/or RH. As shown in Figure 4, strong positive correlations were observed between pH and the mass concentrations of the total aqueous-phase ions at SPB ($r = 0.75$, $p < 0.01$) and JY ($r = 0.78$, $p < 0.01$). This suggests that the hygroscopic growth of aerosols could be related to the reduction of their acidic characteristics [30].

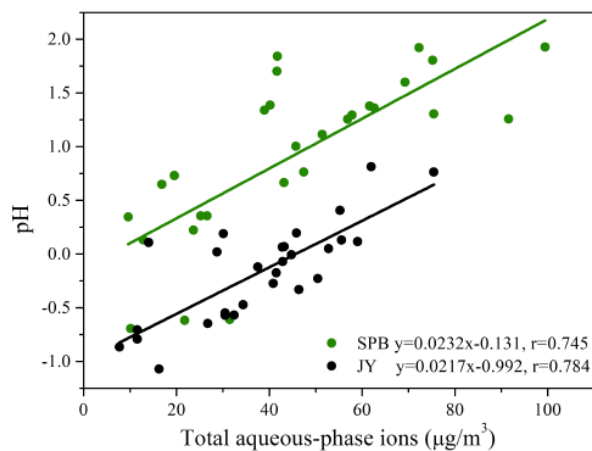


Figure 4: pH as a function of the total aqueous-phase ions.

As illustrated in Table 2, $[\text{H}^+]_{\text{total}}$ was generally equal to the sum of $[\text{H}^+]_{\text{in-situ}}$ and $[\text{HSO}_4^-]$, indicating nearly all of the hydrogen ions existed in the aqueous-phase. The contribution of $[\text{H}^+]_{\text{in-situ}}$ to $[\text{H}^+]_{\text{total}}$ at SPB and JY varied widely (19.0% and 45.8%, respectively). As shown in Figure 3 (c), the concentration of NH_4^+ was relatively lower at JY, with NH_4^+ and SO_4^{2-} mainly in the form of NH_4HSO_4 rather than $(\text{NH}_4)_2\text{SO}_4$. Thus, more HSO_4^- might be present at JY site, facilitating HSO_4^- dissociation into H^+ and SO_4^{2-} . Conversely, higher concentration of SO_4^{2-} at SPB might inhibit the dissociation of HSO_4^- into H^+ . Consequently, both the concentration and contribution of $[\text{H}^+]_{\text{in-situ}}$ at JY were higher than those at SPB.

3.4. Formation Mechanisms of SO_4^{2-} and NO_3^-

The concentrations of SO_4^{2-} and NO_3^- in $\text{PM}_{2.5}$ are mainly determined by the concentrations of their precursors (SO_2 and NO_2) and the conversion rate in the atmosphere. Generally, SO_4^{2-} and NO_3^- formation from precursors can be indicated by sulfur oxidation ratio (SOR) and nitrogen oxidation ratio (NOR) [3, 31]. The SOR and NOR are defined as follows,

$$\text{SOR} = [\text{SO}_4^{2-}] / ([\text{SO}_4^{2-}] + \text{SO}_2) \quad (6)$$

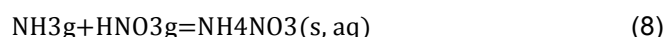
$$\text{NOR} = \text{NO}_3^- / (\text{NO}_3^- + \text{NO}_2) \quad (7)$$

where the mole concentrations (mol/m³) of all the parameters were used. Higher SOR and NOR indicate more secondary oxidation of SO₂ and NO₂.

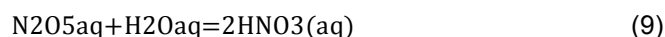
Due to the lack of SO₂ and NO₂ data at YB site, only the oxidation ratios at the other three sites were calculated. Average SOR were 0.30±0.10, 0.26±0.08, 0.30±0.12, and NOR were 0.07±0.04, 0.13±0.06, 0.08±0.03 at JFB, JY and SPB, respectively. Previous studies proposed that when SOR was higher than 0.10, photochemical oxidation of SO₂ would occur in the atmosphere, but when SOR was lower than 0.10, SO₄²⁻ was mainly attributed by the primary emissions [3, 32]. In our study, SOR was much higher than 0.10 among the three sampling sites, implying the secondary formation of SO₄²⁻ from SO₂ in Chongqing. There are two formation mechanisms for SO₄²⁻ from SO₂ in the troposphere, including homogeneous gas-phase and heterogeneous reactions in the aqueous surface layer of pre-existing particles [17, 33]. Meanwhile, heterogeneous reactions tend to be the most important formation mechanism of SO₄²⁻ under high relative humidity condition (RH>75%) [34]. As shown in Table 2, the average RH was above 75% in all the sites except for JFB (68.7%), suggesting that the heterogeneous reactions may play a dominate role in the formation of SO₄²⁻ in Chongqing. In addition, the correlation coefficients between SOR, NOR and the related parameters were summarized in Table 4. The correlation between SOR and PM_{2.5} mass was higher compared to that between SOR and other parameters, demonstrating the secondary formation of sulfate contributed greatly to the increase of PM_{2.5} concentration.

The NOR values were lower than 0.1 at SPB and JFB, but higher than 0.1 at JY site (0.13). The relatively low NOR values at the two urban sites could be related to the high temperature (~20 °C) during the sampling

period, which is not favorable to the formation of particulate NH₄NO₃. Positive correlations were found between NOR and SO₄²⁻ at JFB and SPB sites (Table 4), suggesting that the formation of secondary NO₃⁻ might be related to SO₄²⁻ in the atmosphere. Tian *et al.* [35] have reported that SO₄²⁻ may promote the formation of NO₃⁻. Additionally, the good correlations between NOR and RH (r=0.44–0.70, p<0.05) indicates that the conversion of NO₂ to NO₃⁻ might be influenced by RH. There are two major pathways for the formation of nitrate. The first pathway is the homogenous gas-phase reaction:



And the second pathway is the heterogeneous hydrolysis of N₂O₅ on the pre-existing aerosols:



In the SO₄²⁻-NH₄⁺-NO₃⁻ thermodynamic system, SO₄²⁻ competes with NO₃⁻ for NH₄⁺ during the formation of NO₃⁻. Therefore, the relationship between molar ratio of nitrate to sulfate ([NO₃⁻]/[SO₄²⁻]) and that of ammonium to sulfate ([NH₄⁺]/[SO₄²⁻]) is often used to indicate the pathway of NO₃⁻ formation [29, 31]. Generally, linear correlation between these two ratios in NH₄⁺-rich condition ([NH₄⁺]/[SO₄²⁻]>1.5) suggests the homogeneous formation of NO₃⁻ [2, 36].

[NO₃⁻]/[SO₄²⁻] is plotted against [NH₄⁺]/[SO₄²⁻] at the four sites of Chongqing, as shown in Figure 5(a). Significant correlation (r=0.86, p<0.01) was found between them at the three urban sites with sufficient ammonium, suggesting homogeneous reaction was a significant pathway for nitrate formation in urban Chongqing [29, 31]. But obviously, poor correlation (r=0.29, p<0.05) was observed at the rural site, which may be attributed to the high acidity at JY site, promoting the heterogeneous hydrolysis of N₂O₅ [37-

Table 4: Correlation Coefficients between SOR, NOR and other Related Parameters

		PM _{2.5}	SO ₂	RH	T	O ₃
SOR	JFB	0.660**	-0.218	0.384*	0.457*	0.112
	SPB	0.604**	-0.479**	0.343	0.471**	0.338
	JY	0.578**	-0.446*	0.103	0.491**	0.477*
		PM _{2.5}	NO ₂	SO ₄ ²⁻	RH	T
NOR	JFB	0.317	-0.134	0.420*	0.695*	-0.378*
	SPB	0.347	-0.256	0.487**	0.585**	-0.330
	JY	0.426*	-0.109	0.361	0.439**	-0.054

**Correlation is significant at the 0.01 level,*Correlation is significant at the 0.05 level.

39]. The regression function was $[\text{NO}_3^-]/[\text{SO}_4^{2-}] = [\text{NH}_4^+]/[\text{SO}_4^{2-}] \times 0.739 - 1.076$ for the three urban sites, and the intercept of the regression line with the axis of $[\text{NH}_4^+]/[\text{SO}_4^{2-}]$ was 1.46. Thus, the excess NH_4^+ associated with the formation of NO_3^- can be derived from the following equation:

$$[\text{NH}_4^+]_{\text{excess}} = ([\text{NH}_4^+]/[\text{SO}_4^{2-}] - 1.46) \times [\text{SO}_4^{2-}] \quad (10)$$

As illustrated in Figure 5(b), the concentration of excess ammonium was mostly higher than 0 and linearly correlated with nitrate in urban Chongqing, indicating that the nitrate increased with the excess ammonium via homogeneous reaction of NH_3 and HNO_3 in the atmosphere. It further implies that the gas-phase homogeneous reaction was mainly responsible for the formation of NO_3^- in those areas [31, 35]. The regression slope (0.58) was lower than 1, indicating

that approximately 58% excess ammonium was bound formed nitrate salts of ammonium. The remaining excess ammonium was bound to the species other than nitrate, such as chloride.

3.5. Analysis of Regional Transport

To further understand the impact of regional transport on Chongqing, a trajectory clustering method was used to examine the pathway of air masses and to investigate the chemical composition among the air masses with different origination, a method that has been used in previous studies [13, 35]. The 48-hour backward trajectories during the sampling period were grouped into four clusters (Figure 6). Meanwhile, the concentrations of $\text{PM}_{2.5}$ and major WSIs in JFB site influenced by each cluster were also depicted in Figure 6.

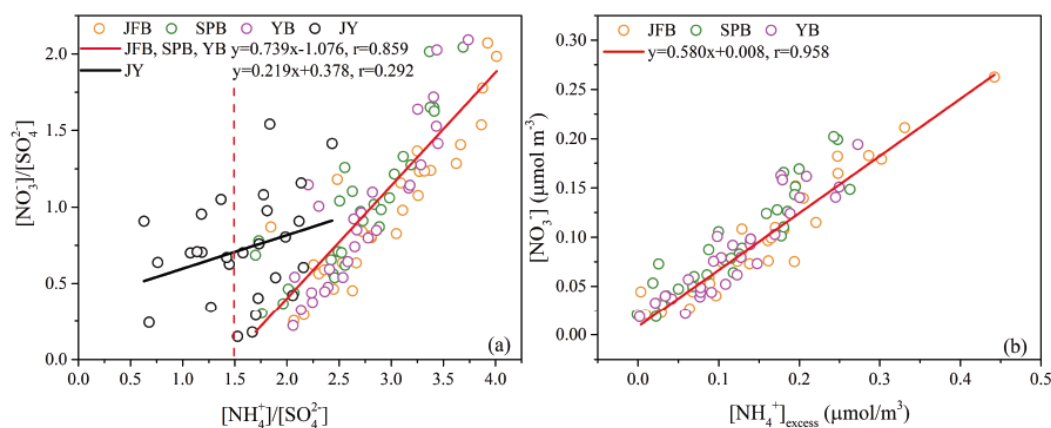


Figure 5: (a) Molar ratios of $[\text{NO}_3^-]/[\text{SO}_4^{2-}]$ versus $[\text{NH}_4^+]/[\text{SO}_4^{2-}]$ at urban and rural sites of Chongqing, (b) Molar concentrations of $[\text{NO}_3^-]$ versus $[\text{NH}_4^+]_{\text{excess}}$.

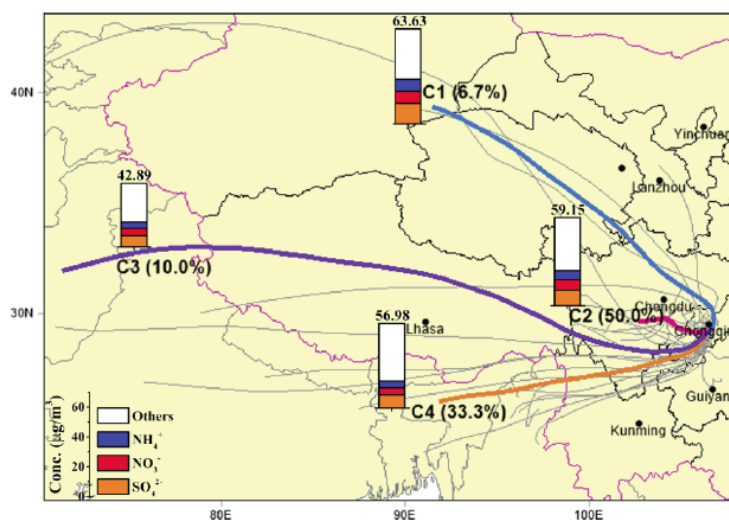


Figure 6: Clusters of air mass backward trajectories arriving at 300 m above ground level in Chongqing for 15 October to 13 November. The numbers above the bar stand for the average concentrations of $\text{PM}_{2.5}$ in each cluster. "Others" represents the composition of $\text{PM}_{2.5}$ except for SNA.

The air masses reaching urban Chongqing in autumn mainly came from west direction, including northwest, west and southwest. The northwest air mass corresponded to a middle-distance cluster 1, accounting for 6.7% of the total trajectories with highest PM_{2.5} (average: 63.6 µg/m³) and SO₄²⁻ (average: 13.7 µg/m³) concentrations. This polluted air mass originated from Xinjiang Uighur Autonomous Region and passed through Qinghai Province, then entered the northwest of Sichuan Basin. The air mass from the west included short-distance cluster 2 and long-distance cluster 3, accounting for 50.0% and 10.0% of the total trajectories, respectively. The short-distance cluster 2 from the west can be attributed to the areas within the basin, including neighboring Chengdu Plain, known as a heavily polluted area in China [40]. Meanwhile, the trajectory length of cluster 2 was very short, hovering in the Sichuan Basin for a long time, favoring the accumulation of pollutants. As a consequence, PM_{2.5} (average: 59.2 µg/m³) and SNA concentrations were second highest under the influence of cluster 2. In contrast, the lowest PM_{2.5} concentration (average: 42.9 µg/m³) was observed in long-distance cluster 3 from the far west, which originated in Pakistan, passed through Tibet Plateau and entered Sichuan Province via Western Sichuan Plain. The southwest air mass corresponded to a middle-distance cluster 4, accounting for 33.3% of the total trajectories. Cluster 4 originated from India, and passed through Burma, Yunnan and south of Sichuan Province, corresponding to moderate PM_{2.5} concentrations (average: 57.0 µg/m³) during this period.

4. CONCLUSIONS

Mass concentration and the water-soluble inorganic ions and site-to-site variations of the PM_{2.5} data among four sites of Chongqing were examined. The PM_{2.5} mass concentrations at the urban sites were 62.8–73.0% higher than that at the rural site. The total ions accounted for about 38.8–40.8% of PM_{2.5} at urban sites and 43.5% of PM_{2.5} at the rural site. Severe secondary aerosol pollution was suggested by the high contribution of SNA (>90%) in Chongqing. The spatial distribution analysis of SNA among the four sites suggested that the process of accumulation and removal of SO₄²⁻ might be similar throughout different urban areas in Chongqing. Additionally, SNA were mainly present in the forms of (NH₄)₂SO₄ and NH₄NO₃ at the urban sites, while they were in the forms of NH₄HSO₄ and NH₄NO₃ at the rural site.

PM_{2.5} was more acidic at the rural site than the urban sites. The better correlation between SOR and PM_{2.5} mass and the high RH during the sampling period suggested heterogeneous process dominated the formation of SO₄²⁻. Though homogeneous reaction dominated the formation of NO₃⁻ at the urban sites, heterogeneous reactions occurred at the rural site. Trajectory analysis suggested that aerosol pollution in Chongqing was mostly influenced by air masses originating from local areas.

ACKNOWLEDGMENTS

This work was supported by National Key R&D Program of China (No. 2018YFC0214004), and the National Natural Science Foundation of China (No. 41375123, 41405027 and 41403089). We thank Jia Liu, Jinsheng Zhu, Jun Wang, Xin Zhao, Xueyong Shen, Yue Yuan, Jing Cui, Min He, Qin Li, Qing Gu, Ying Fang and Yuan Liu for their assistance in PM_{2.5} sampling. The authors declare no conflict of interest.

REFERENCES

- [1] Zheng S, Pozzer A, Cao CX, Lelieveld J. Long-term (2001–2012) fine particulate matter (PM_{2.5}) and the impact on human health in Beijing, China. *Atmospheric Chemistry & Physics* 2015; 14(21): 28657–28684. <https://doi.org/10.5194/acpd-14-28657-2014>
- [2] He K, Zhao Q, Ma Y, Duan F, Yang F, Shi Z. *et al.*, Spatial and seasonal variability of PM_{2.5} acidity at two Chinese megacities: insights into the formation of secondary inorganic aerosols. *Atmos Chem Phys* 2012; 12(3): 1377–1395. <https://doi.org/10.5194/acp-12-1377-2012>
- [3] Wang Y, Zhuang GS, Tang AH, Yuan H, Sun YL, Chen SA. *et al.*, The ion chemistry and the source of PM_{2.5} aerosol in Beijing. *Atmos Environ* 2005; 39(21): 3771–3784. <https://doi.org/10.1016/j.atmosenv.2005.03.013>
- [4] Tian M, Wang H, Chen Y, Zhang L, Shi G, Liu Y *et al.*, Highly time-resolved characterization of water-soluble inorganic ions in PM_{2.5} in a humid and acidic mega city in Sichuan Basin, China. *Science of The Total Environment* 2017; 580: 224–234. <https://doi.org/10.1016/j.scitotenv.2016.12.048>
- [5] Bao Z, Chen L, Li K, Han L, Wu X, Gao X *et al.*, Meteorological and chemical impacts on PM_{2.5} during a haze episode in a heavily polluted basin city of eastern China. *Environmental Pollution* 2019; 250: 520–529. <https://doi.org/10.1016/j.envpol.2019.04.045>
- [6] Hu GY, Zhang YM, Sun JY, Zhang LM, Shen XJ, Lin WL *et al.*, Variability, formation and acidity of water-soluble ions in PM_{2.5} in Beijing based on the semi-continuous observations. *Atmos Res* 2014; 145: 1–11. <https://doi.org/10.1016/j.atmosres.2014.03.014>
- [7] Lai SC, Zou SC, Cao JJ, Lee SC, Ho KF. Characterizing ionic species in PM_{2.5} and PM₁₀ in four Pearl River Delta cities, South China. *J Environ Sci-China* 2007; 19(8): 939–947. [https://doi.org/10.1016/S1001-0742\(07\)60155-7](https://doi.org/10.1016/S1001-0742(07)60155-7)
- [8] Huang RJ, Zhang YL, Bozzetti C, Ho KF, Cao JJ, Han YM *et al.*, High secondary aerosol contribution to particulate pollution during haze events in China. *Nature* 2014;

- 514(7521): 218-222.
<https://doi.org/10.1038/nature13774>
- [9] Fu XX, Guo H, Wang XM, Ding X, He QF, Liu TY *et al.*, PM_{2.5} acidity at a background site in the Pearl River Delta region in fall-winter of 2007-2012. *J Hazard Mater* 2015; 286: 484-492.
<https://doi.org/10.1016/j.jhazmat.2015.01.022>
- [10] Chongqing Municipal Bureau of Statistics. Chongqing Statistics Yearbook (2015).
<http://tjj.cq.gov.cn/tjnj/2015/indexch.htm>
- [11] General Office of the State Council of the People's Republic of China. Air Pollution Prevention and Control Action Plan. http://www.mee.gov.cn/gzfw_13107/zcfg/hjjzc/gjfbdjzcx/hjczc/201606/t20160623_355606.shtml
- [12] Nation Bureau of Statistics of China. National Statistics Yearbook (2015).
<http://www.stats.gov.cn/tjsj/ndsj/2015/indexch.htm>
- [13] Peng C, Tian M, Chen Y, Wang H, Zhang L, Shi G *et al.*, Characteristics, Formation Mechanisms and Potential Transport Pathways of PM_{2.5} at a Rural Background Site in Chongqing, Southwest China. *Aerosol and Air Quality Research* 2019; 19(9): 1980-1992.
<https://doi.org/10.4209/aaqr.2019.01.0010>
- [14] Karthikeyan S, Balasubramanian R. Determination of water-soluble inorganic and organic species in atmospheric fine particulate matter. *Microchem J* 2006; 82(1): 49-55.
<https://doi.org/10.1016/j.microc.2005.07.003>
- [15] Wang H, Tian M, Chen Y, Shi G, Liu Y, Yang F *et al.*, Seasonal characteristics, formation mechanisms and source origins of PM_{2.5} in two megacities in Sichuan Basin, China. *Atmos. Chem. Phys* 2018; 18(2): 865-881.
<https://doi.org/10.5194/acp-18-865-2018>
- [16] Zhang ZQ, Friedlander SK. A comparative study of chemical databases for fine particle Chinese. *Environ Sci Technol* 2000; 34(22): 4687-4694.
<https://doi.org/10.1021/es001147t>
- [17] Meng CC, Wang LT, Zhang FF, Wei Z, Ma SM, Ma X *et al.*, Characteristics of concentrations and water-soluble inorganic ions in PM_{2.5} in Handan City, Hebei province, China. *Atmos Res* 2016; 171: 133-146.
<https://doi.org/10.1016/j.atmosres.2015.12.013>
- [18] Extended AIM Aerosol Thermodynamics Model II. <http://www.aim.env.uea.ac.uk/aim/model2/model2a.php>
- [19] Clegg SL, Brimblecombe P, Wexler AS. Thermodynamic model of the system H⁺-NH₄⁺-Na⁺-SO₄²⁻-NO₃⁻-Cl⁻-H₂O at 298.15 K. *J Phys Chem A* 1998; 102(12): 2155-2171.
<https://doi.org/10.1021/jp973043j>
- [20] Zhang Q, Jimenez JL, Worsnop DR, Canagaratna M. A case study of urban particle acidity and its influence on secondary organic aerosol. *Environ Sci Technol* 2007; 41(9): 3213-3219.
<https://doi.org/10.1021/es061812j>
- [21] Wang YQ, Zhang XY, Draxler RR. Traj Stat: GIS-based software that uses various trajectory statistical analysis methods to identify potential sources from long-term air pollution measurement data. *Environmental Modelling & Software* 2009; (8): 938-939.
<https://doi.org/10.1016/j.envsoft.2009.01.004>
- [22] Song M, Liu X, Tan Q, Feng M, Qu Y, An J *et al.*, Characteristics and formation mechanism of persistent extreme haze pollution events in Chengdu, southwestern China. *Environmental Pollution* 2019; 251: 1-12.
<https://doi.org/10.1016/j.envpol.2019.04.081>
- [23] National Oceanic and Atmospheric Administration (NOAA) Air Resource Laboratory Archived Global Data Assimilation System (GDAS). <ftp://arlftp.arlhq.noaa.gov/pub/archives/>
- [24] Zhao Q. Characteristics and Formation of Inorganic Fine Particulate Pollution in Typical Regions of China. Ph. D. Thesis, Tsinghua University, China 2010.
- [25] Wang H, Qiao B, Zhang L, Yang F, Jiang X. Characteristics and sources of trace elements in PM_{2.5} in two megacities in Sichuan Basin of southwest China. *Environmental Pollution* 2018; 242: 1577-1586.
<https://doi.org/10.1016/j.envpol.2018.07.125>
- [26] Chen Y, Xie S, Luo B, Zhai C. Particulate pollution in urban Chongqing of southwest China: Historical trends of variation, chemical characteristics and source apportionment. *Science of The Total Environment* 2017; 584: 523-534.
<https://doi.org/10.1016/j.scitotenv.2017.01.060>
- [27] Chongqing Ecology and Environment Bureau. Report on the State of Environment in Chongqing (2015). <http://sthjj.cq.gov.cn/uploadfiles/201601/26/2016012610285060265652.pdf>
- [28] Ianniello A, Spataro F, Esposito G, Allegrini I, Hu M, Zhu T. Chemical characteristics of inorganic ammonium salts in PM_{2.5} in the atmosphere of Beijing (China). *Atmos. Chem. Phys.* 2011; 11(21): 10803-10822.
<https://doi.org/10.5194/acp-11-10803-2011>
- [29] Pathak RK, Wu WS, Wang T. Summertime PM_{2.5} ionic species in four major cities of China: nitrate formation in an ammonia-deficient atmosphere. *Atmospheric Chemistry and Physics* 2009; 9(5): 1711-1722.
<https://doi.org/10.5194/acp-9-1711-2009>
- [30] Behera SN, Cheng JP, Balasubramanian R. In situ acidity and pH of size-fractionated aerosols during a recent smoke-haze episode in Southeast Asia. *Environ Geochem Health* 2015; 37(5): 843-859.
<https://doi.org/10.1007/s10653-014-9660-1>
- [31] Jansen RC, Shi Y, Chen JM, Hu YJ, Xu C, Hong SM *et al.*, Using hourly measurements to explore the role of secondary inorganic aerosol in PM_{2.5} during haze and fog in Hangzhou, China. *Adv Atmos Sci* 2014; 31(6): 1427-1434.
<https://doi.org/10.1007/s00376-014-4042-2>
- [32] Ohta S, Okita T. A chemical characterization of atmospheric aerosol in Sapporo. *Atmospheric Environment. Part A. General Topics* 1990; 24(4): 815-822.
[https://doi.org/10.1016/0960-1686\(90\)90282-R](https://doi.org/10.1016/0960-1686(90)90282-R)
- [33] Wang Y, Zhuang GS, Sun YL, An ZS. The variation of characteristics and formation mechanisms of aerosols in dust, haze, and clear days in Beijing. *Atmos Environ* 2006; 40(34): 6579-6591.
<https://doi.org/10.1016/j.atmosenv.2006.05.066>
- [34] McMurry PH, Wilson JC. Droplet Phase (Heterogeneous) and Gas-Phase (Homogeneous) Contributions to Secondary Ambient Aerosol Formation as Functions of Relative Humidity. *J Geophys Res-Oc Atm* 1983; 88(Nc9): 5101-5108.
<https://doi.org/10.1029/JC088iC09p05101>
- [35] Tian M, Wang HB, Chen Y, Yang FM, Zhang XH, Zou Q *et al.*, Characteristics of aerosol pollution during heavy haze events in Suzhou, China. *Atmos Chem Phys* 2016; 16(11): 7357-7371.
<https://doi.org/10.5194/acp-16-7357-2016>
- [36] Huang XF, Qiu R, Chan CK, Kant PR. Evidence of high PM_{2.5} strong acidity in ammonia-rich atmosphere of Guangzhou, China: Transition in pathways of ambient ammonia to form aerosol ammonium at [NH₄⁺]/[SO₄²⁻] = 1.5. *Atmospheric Research* 2011; 99(3): 488-495.
<https://doi.org/10.1016/j.atmosres.2010.11.021>
- [37] Kaiser HF. Citation-Classic - the Application of Electronic-Computers to Factor-Analysis. *Cci/Soc Behav Sci* 1986; (40): 18-18.
- [38] Pathak RK, Louie PKK, Chan CK. Characteristics of aerosol acidity in Hong Kong. *Atmos Environ* 2004; 38(19): 2965-2974.
<https://doi.org/10.1016/j.atmosenv.2004.02.044>
- [39] Xue J, Lau AKH, Yu JZ. A study of acidity on PM_{2.5} in Hong Kong using online ionic chemical composition measurements. *Atmos Environ* 2011; 45(39): 7081-7088.
<https://doi.org/10.1016/j.atmosenv.2011.09.040>

[40] Tao J, Zhang L, Cao J, Zhang R. A review of current knowledge concerning PM_{2.5} chemical composition, aerosol optical properties and their relationships across

China. Atmos. Chem. Phys 2017; 17(15): 9485-9518.
<https://doi.org/10.5194/acp-17-9485-2017>

Received on 30-11-2019

Accepted on 2-1-2020

Published on 10-1-2020

DOI: <https://doi.org/10.12974/2311-8741.2020.08.2>

© 2020 Song *et al.*; Licensee Savvy Science Publisher.

This is an open access article licensed under the terms of the Creative Commons Attribution Non-Commercial License (<http://creativecommons.org/licenses/by-nc/3.0/>) which permits unrestricted, non-commercial use, distribution and reproduction in any medium, provided the work is properly cited.